Estimation of the tangential stresses in the stator/ rotor contact of travelling wave ultrasonic motors using visco-elastic foundation models

X. Cao, J. Wallaschek
Heinz Nixdorf Institute, University of Paderborn, Pohlweg 47-49, D-33098 Paderborn, Germany

Abstract

A new stator/rotor contact model of travelling wave ultrasonic motors is developed, in which the stick/slip behavior within the contact area is taken into account. The distributions of displacement and velocity and normal and tangential interface forces between rotor and stator are calculated. The results allow to estimate motor performance like e.g. the torque-speed curves as a function of the motor's parameters. Furthermore, the influence of main material and geometrical parameters and different operating conditions are investigated. The mathematical model developed in this paper can be used as a design tool for optimizing motor performance with the flexibility for a wide variety of geometries and materials.

1 Introduction

Travelling wave ultrasonic motors are a new type of small scale actuators. They have been attracting considerable attention in industry because of their unique characteristics such as high torque, low speed, compact size, silence and good controllability.

In these motors, electrical energy is transformed to high-frequency mechanical oscillation by means of piezoelectric elements. The stator of the motor oscillates in such a way that material points on the stator surface perform an elliptical motion. The rotor is pressed to the stator and is driven by the frictional forces generated in the contact area between them. This working principle has been described in detail in several publications[1-4]. Although the travelling wave ultrasonic motor was invented more than ten years ago and has now been

investigated for quite a while, some few fundamental phenomena are still not well understood. The most important and most difficult problems are related to the stator/rotor contact. The stator/ rotor contact displays inherently non-linear dynamic characteristics which are very important for understanding and designing the motor performance[4,5].

In this paper a new stator/rotor contact model is developed, in which the surface layer on the rotor is modelled as a series of mass-visco/elastic springs. The stick/slip behavior within the contact area is taken into account.

2 Contact model

Figure 1 shows a travelling wave ultrasonic motor. In the stator travelling bending waves are excited by piezoelectric elements so that the deflection of the middle surface of the stator is given by

$$w(r,\varphi,t) = R(r)\cos(\omega\, t - k\varphi), \qquad (1)$$

where k is the number of nodal diameters, ω is the circular frequency of vibration and $R(r)$ is a function describing the radial dependence of the vibration amplitude[3]. The rotor of the travelling wave ultrasonic motor consists of a plate and a thin contact layer bonded to the rotor surface. The rotor is driven by tangential stresses between the vibrating stator and rotor. In this paper a visco-elastic foundation model is used to simulate the stator/rotor contact , in which the surface layer on the rotor is modelled as a series of mass-visco/elastic springs (Fig. 2).

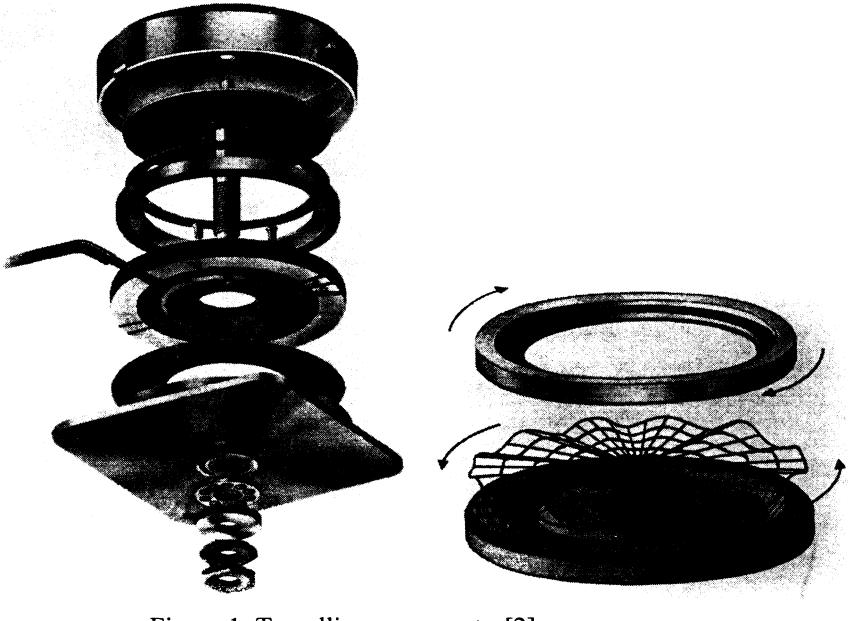

Figure 1 Travelling wave motor[2].

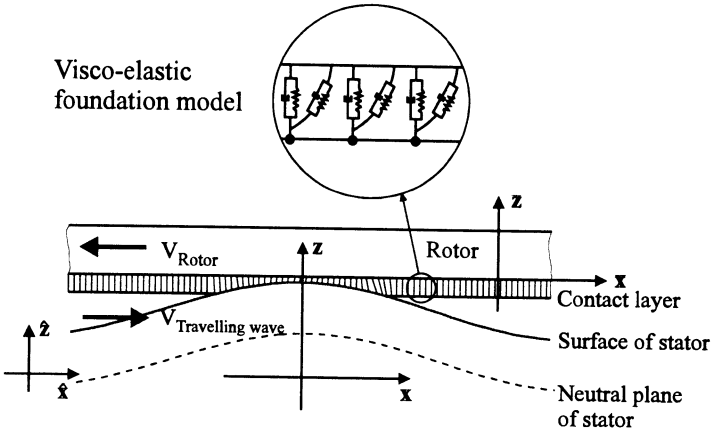

Figure 2 Stator/rotor contact model and its coordinate systems

3. Analysis of the stator/rotot contact

For simplicity, the circular geometry will be replaced by a linear one. Since the width of the contact layer is significantly smaller than its length, the problem can be further reduced to a two-dimensional problem. The deflection of the middle plane of the stator is then given in a rectangular coordinate system $(\hat{x},\hat{z})$ by

$$w(\hat{x},t) = A\cos(\omega\, t - 2\pi\frac{\hat{x}}{\lambda}) \tag{2}$$

where A is the vibration amplitude and λ denotes the wavelength.
To overcome the problem of small deformation in the contact areas superimposed with large travelling wave and rotor motions it is effective to introduce two moving reference frames (x,z) and $(\bar{x},\bar{z})$. The coordinates (x,z) are located at the travelling wave and the coordinates $(\bar{x},\bar{z})$ at the rotor, see Fig.2. The corresponding transformations are:

$$x = \hat{x} - v_w t \quad \text{with} \quad v_w = \frac{\lambda}{2\pi}\omega\,, \tag{3}$$

$$\bar{x} = \hat{x} - v_R t \tag{4}$$

and

$$\bar{x} = x + v\,t \quad \text{with} \quad v = v_w - v_R \tag{5}$$

where v_w is the velocity of the travelling wave and v_R is the tangential velocity of the rotor. In the coordinates (x,z) the deflection of the middle surface of the stator becomes stationary

$$w(x) = A\cos\frac{2\pi}{\lambda}x\,. \tag{6}$$

Using Kirchhoff's plate theory the tangential velocity of the stator's surface is given by

$$v_s(x) = -\frac{2\pi A}{\lambda}\frac{2\pi a}{\lambda} v_w \cos\frac{2\pi x}{\lambda}, \tag{7}$$

where a is the distance between the neutral plane and the surface of the stator.

The rotor can be regarded as a rigid strip moving with velocity v_R. The tangential velocity of the surface points in the contact layer is expressed as

$$v_r(\hat{x},t) = v_R + v_{rr}(\bar{x},t), \tag{8}$$

where v_{rr} is the deformation velocity of material points on the contact layer's surface relative to the rotor. Using elasticity theory and the transformation of the coordinate systems, v_r can be given in the coordinates (x,z) by

$$v_r(x) = v_R + h\varepsilon_x'(x)v, \tag{9}$$

where ε_x is the tangential stress in the contact layer.

The rotor is pressed to the stator by a given normal force, F_{Nb} per unit wavelength. This contact condition creates a normal pressure distribution $p(x)$ at the contact area which is

$$p(x) = E\varepsilon_z(x) = \frac{EA}{h}(\cos 2\pi\frac{x}{\lambda} - \cos 2\pi\frac{L}{\lambda}), \text{ for } -L \le x \le L, \tag{10}$$

where L is the length of the contact area. It can be determined from the condition that the force is equal to the integral of the pressure distribution over the contact area:

$$F_{Nb} = b\frac{EA}{h}\int_{-L}^{L}(\cos 2\pi\frac{x}{\lambda} - \cos 2\pi\frac{L}{\lambda})dx. \tag{11}$$

In the analysis of the tangential stresses τ of the stator/rotor contact interface Coulomb's friction law is assumed, i.e.:

$$\text{stick:} \quad |\tau| \le \mu_0 p \quad , \quad v_{rel} = 0, \tag{12}$$

$$\text{slip:} \quad |\tau| = \mu p \quad , \quad v_{rel} \ne 0, \tag{13}$$

where μ_0 and μ are the static and dynamic coefficients of friction respectively, and v_{rel} is the relative velocity

$$v_{rel}(x) = v_r(x) - v_s(x). \tag{14}$$

In slip zones, the tangential stress is known from the friction law (13):

$$\tau(x) = -sign(v_{rel})\mu\, p(x) = -sign(v_{rel})\frac{\mu EA}{h}(\cos 2\pi\frac{x}{\lambda} - \cos 2\pi\frac{L}{\lambda}). \tag{15}$$

The strain in the contact layer can then be determined from the following boundary-value problem:

$$m\ddot{\varepsilon}_{\hat{x}}(\hat{x},t) + \gamma\,\dot{\varepsilon}_{\hat{x}}(\hat{x},t) + G\varepsilon_{\hat{x}}(\hat{x},t) = \tau(\hat{x},t). \tag{16}$$

with appropriate boundary conditions, m, γ, G are the mass, damping and stiffness parameters of the contact layer' material. By using the transformation of the coordinate system, (16) can be solved in (x,z) coordinate system. The solution is:

$$\varepsilon_x(x) = C_1 e^{\bar{\alpha}x}\cos\bar{\beta}x + C_2 e^{\bar{\alpha}x}\sin\bar{\beta}x + \varepsilon_x^*(x), \tag{17}$$

with

$$\bar{\alpha} = \frac{\gamma}{2mv_w}, \quad \bar{\beta} = \frac{1}{v_w}\sqrt{\frac{G}{m}}\sqrt{1-\frac{\gamma^2}{4mG}}, \quad \bar{Q} = -sign(v_{rel})\frac{\mu EA}{h}$$

$$\varepsilon_x^*(x) = \bar{A}\sin 2\pi\frac{x}{\lambda} + \bar{B}\cos 2\pi\frac{x}{\lambda} - \frac{\bar{Q}}{G}\cos 2\pi\frac{L}{\lambda}, \tag{18}$$

$$\bar{A} = \frac{-\gamma v_w \frac{2\pi}{\lambda}\bar{Q}}{G^2 + (\gamma^2 - 2Gm)v_w^2\frac{4\pi^2}{\lambda^2} + (mv_w^2\frac{4\pi^2}{\lambda^2})^2}, \tag{19}$$

$$\bar{B} = \frac{(G - mv_w^2\frac{4\pi^2}{\lambda^2})\bar{Q}}{G^2 + (\gamma^2 - 2Gm)v_w^2\frac{4\pi^2}{\lambda^2} + (mv_w^2\frac{4\pi^2}{\lambda^2})^2}. \tag{20}$$

Both integral constants C_1 and C_2 can be determind from the boundary conditions. Finally, the tangential velocity of the surface points of the contact layer in slip zones can be obtained from (9).

In stick zones, v_r is known from the kinematic condition

$$v_r(x) = v_s(x). \tag{21}$$

From (7) and (9) we obtain

$$\varepsilon_x'(x) = -\frac{1}{hv}v_R - \frac{aA4\pi^2 v_w}{h\lambda^2 v}\cos 2\pi\frac{x}{\lambda} \tag{22}$$

and the tangential stress can be determined from

$$\tau(x) = mv_w^2\varepsilon_x''(x) + \gamma v_w\varepsilon_x'(x) + G\varepsilon_x(x). \tag{23}$$

The tangential stress in stick zones, i.e. the solution of (23), is

$$\tau(x) = -\frac{\gamma v_w}{hv}v_R - \frac{Gv_R}{hv}x - \frac{aA4\pi^2\gamma v_w^2}{h\lambda^2 v}\cos 2\pi\frac{x}{\lambda} + \tag{24}$$

$$-\frac{aAGv_w 2\pi}{h\lambda v}(1 - \frac{4\pi^2 m v_w^2}{\lambda^2 G})\sin 2\pi\frac{x}{\lambda} + GD_i.$$

The integral constant D_i can be determined from the boundary condition

$$\tau(\zeta_i)_{stick} = \tau(\zeta_i)_{slip}, \tag{25}$$

where $x = \zeta_i$ is the boundary point between slip and stick zones. From (25),(24) and (15) D_i is obtained as:

$$D_i = \frac{\gamma\, v_w}{h v G} v_R + \frac{v_R}{h v}\zeta_i + \frac{aA4\pi^2\gamma\, v_w^2}{h\lambda^2 v G}\cos 2\pi\frac{\zeta_i}{\lambda} + \frac{aAv_w 2\pi}{h\lambda v}(1 - \frac{4\pi^2 m}{\lambda^2 G} v_w^2)\sin 2\pi\frac{\zeta_i}{\lambda}$$
$$-sign(v_{rel})\mu\frac{EA}{Gh}(\cos 2\pi\frac{\zeta_i}{\lambda} - \cos 2\pi\frac{L}{\lambda}). \tag{26}$$

4. Numerical results

In this section, a typical travelling wave ultrasonic motor[2] is analyzed as an example of the proposed contact model and formulations.

Tangential velocity fields and stress distributions

Figure 3 a(1-4) gives the tangential velocity fields for different rotor velocities v_R. The relative tangential contact stress distributions are shown in figure 3 b(1-4). When the rotor velocity v_R is very small, e.g. v_R=0, the tangential velocity of the surface points in the contact layer v_r is smaller than the velocity of the corresponding contact points on the surface of the stator and slip does occur in the whole contact area (Fig. 3 a1). In this case, the direction of the tangential contact stress is positive and its value is proportional to the normal force (Fig.3 b1). If v_R is larger, the velocity v_r reaches the same value as v_s before the end of contact. A stick zone occurs in the contact area (Fig.3 a2) and the corresponding tangential stress is smaller than the maximum friction shear stress μp (Fig.3 b2). In a general case, more than one slip and stick zones can be observed in the contact area (Fig.3 a3,b3). At the beginning of contact, v_s is lower than v_r. Consequently, the staor/rotor interface slips at a certain velocity. The direction of the tangential contact stress is negative and the contact layer is braked. Later, when the speeds v_r and v_s become the same, the interface sticks. At this time, the tangential stress is smaller than the maximum friction shear stress. After that, v_s exceeds v_r and the interface slips again. During this slip, the tangential stress has a positive value and the contact layer is accelerated. When both v_r and v_s become the same again, the interface sticks again. Later, v_s becomes lower and again slip occurs. The direction of the tangential stress becomes negative. Finally, the interfaces loose contact. If the rotor velocity is very large (Fig.3 a4), slip is observed in the whole contact area and the tangential contact stress is always negative (Fig.3 b4).

Influence of parameters

The influence of material and geometrical parameters of the motor and different operating conditions can be investigated by using the proposed contact

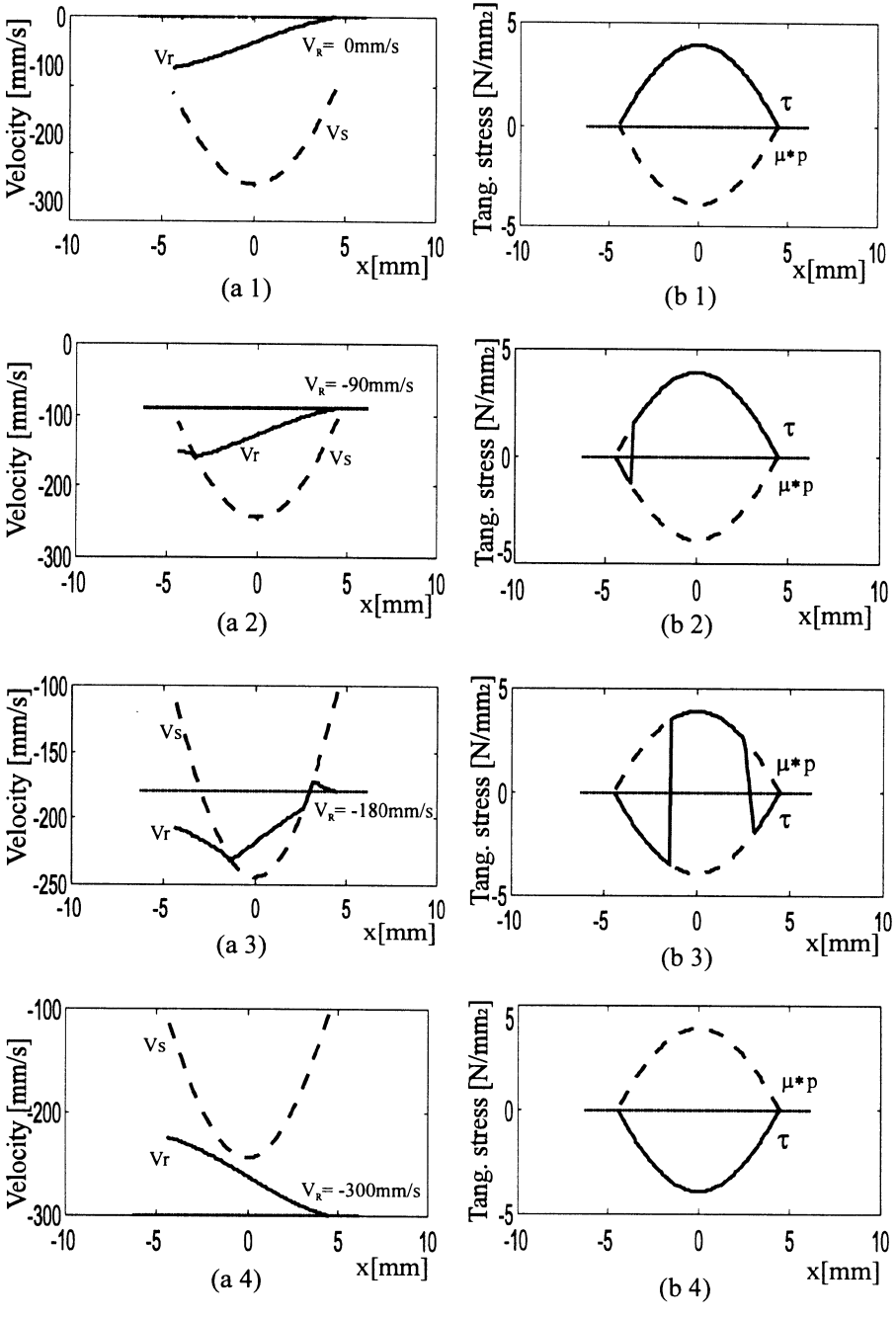

Figure 3 Velocity fields and tangential contact stress distributions for different rotor velocities v_R

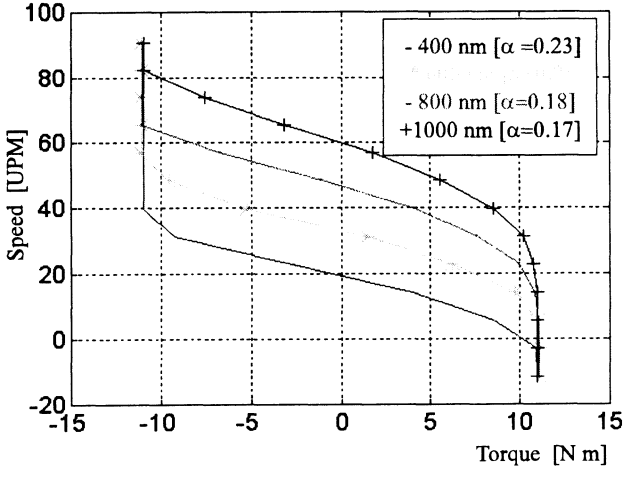

Figure 4:
Torque-speed curves for different stator vibration amplitudes.

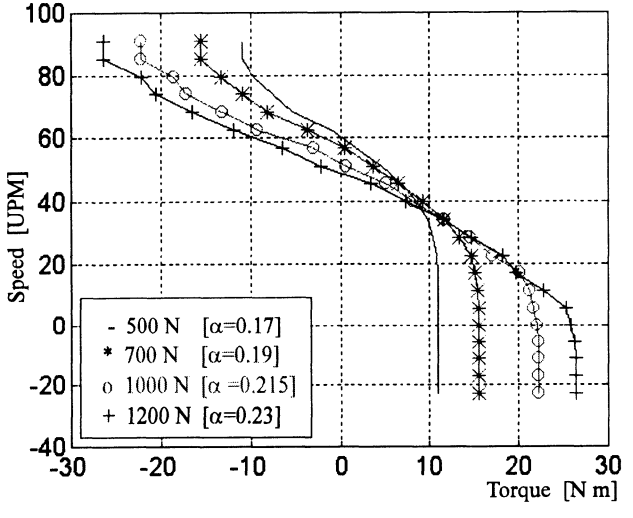

Figure 5:
Torque-speed curves for different applied normal forces.

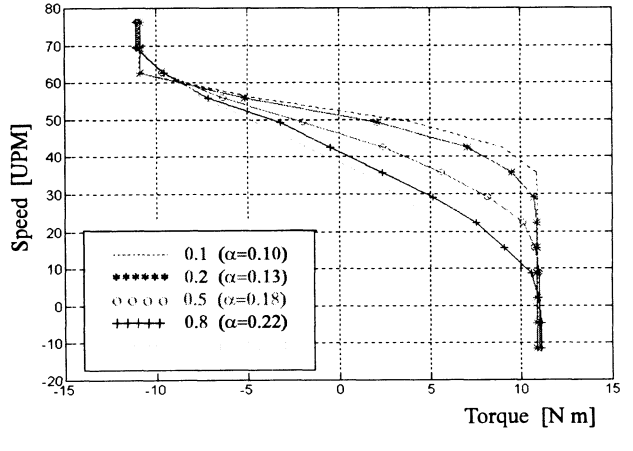

Figure 6:
Torque-speed curves for different thicknesses of contact layer (mm).

model and formulations. The results are illustrated by torque-speed curves as a function of the motor's parameters in the following.

Figure 4 shows the influence of the vibration amplitude of the stator A. We can see that the no-load speed increases proportional with increasing A, but the maximum torque is independent of the amplitude. Figure 5 illustrates the influence of the applied normal force F_N. An increasing F_N creates a large area of contact, i.e. a large value of α (α is the contact length parameter $\alpha = L/\lambda$), and a large maximum torque. The no-load speed however drops with increasing normal forces. Finally figure 6 shows the torque-speed curves for different thickness of the contact layer. In this case the thinner contact layer has a better torque-speed curve and a larger no-load speed. The maximum torque however is independent of the contact layer thickness. All characteristics that have been obtained by the contact model have been observed in travelling wave ultrasonic motors.

5. Conclusions

In this paper a new stator/rotor contact model is developed, which is capable of predicting the tangential velocity fields and tangential stress distributions of the stator/rotor interface and simulating the stick/slip phenomena in the contact area. The influence of main material and geometrical paramers of the motors and different operating conditions have been investigated.

The stator/rotor contact model and the analysis method presented in this paper provide a general approach for modelling travelling wave ultrasonic motors as well as a design tool for optimizing motor performance with the flexibility of allowing for a wide variety of geometries and materials.

References

1. Sashida, T. & Kenjo, T.: *An Introduction to Ultrasonic Motors*. Clarendon Press, Oxford,1993.

2. Schadebrodt, G. & Salomon, B.: Der Piezo-Wanderwellenmotor - ein neues Antriebselement in der Aktorik. 24. *Technisches Presse-Kolloquium der AEG*, 1989.

3. Hagedorn, P. & Wallaschek, J.: Travelling wave ultrasonic motors, part I: Working principle and mathematical modelling of the stator. *Journal of Sound and Vibration* (1992), 155 (1), pp. 31 - 46.

4. Wallaschek, J: Piezoelectric Ultrasonic Motors. Contributed Review Article, to appear in *the Int. Journal of Intelligent Material Systems and Structures*.

5. Maeno, T., Tsukimoto, T. & Miyake, A.: Finite element analysis of the rotor/stator contact in a ring type ultrasonic motor. *IEEE Transactions on Ultrasonics, Ferroelectrics, and Frequency Control*, Vol. 39, No.6,November 1992, pp. 668 - 674.